Performance of FSO Communication Systems Employing Alamouti-Type Space-Time Encoding Over Málaga Channels With Pointing Errors

Abdulgani A. Ibrahim, Serdar Özgür Ata, and Lütfiye Durak-Ata, *Senior Member, IEEE*

***Abstract*—In this work, spatial diversity techniques have been proposed for free-space optical (FSO) communication systems to combat the deteriorating effects, such as atmospheric turbulence effects and pointing errors, and the performance of FSO communication systems with Alamouti encoding scheme over Málaga ($\mathcal{M}$) turbulence channel is investigated. We first derive the probability distribution function (PDF) of end-to-end channel gain under atmospheric turbulence and pointing error circumstances. Then, by capitalizing on this PDF, closed-form expressions of the average bit error rate (BER) and the outage probability (OP) for the proposed system are obtained. Additionally, to provide more insights, the asymptotic expressions for the average BER and the OP are also derived. In the analysis, intensity modulation/direct detection and heterodyne detection techniques are considered so that the obtained results can cover both cases. Furthermore, analytic results are successfully validated through Monte Carlo simulations. Our results highlight the gains in performance that can be achieved when Alamouti encoding scheme is employed in FSO communication systems.**

***Index Terms*—Málaga ($\mathcal{M}$) distribution, atmospheric turbulence, pointing errors, Alamouti encoding, average bit error rate, outage probability.**

I. Introduction

FREE space optical (FSO) communication system is a wireless technology that has gained a considerable attention in the recent past due to its promise to provide the ultra-high data rate required by the fifth-generation (5G) and beyond 5G wireless networks [1]. FSO communication systems also enjoy license-free spectrum, higher security compared to its radio frequency (RF) wireless systems counterpart, low cost, and ease of deployment [2]. However, despite these attractive features, reliability of FSO systems are degraded by weather conditions and atmospheric turbulence effect, which is a result of the random changes in atmospheric temperature, pressure, and altitude. These random changes in the atmosphere, which in return cause variations in refractive index, induce fluctuations of the transmitted optical signal through the atmosphere [3]. Several different distribution models have been proposed to characterize atmospheric turbulence effects encountered in FSO communication links. One of them is the Málaga ($\mathcal{M}$) distribution which has recently received a great attention since it is a generalized form of several widely used models in FSO communication systems such as gamma-gamma, K, and negative exponential distributions that can be expressed as special cases of $\mathcal{M}$ distribution [4]. Another deteriorating effect of the performance of FSO communication systems is the pointing error which is caused by misalignment of the transmitting and receiving apertures in an FSO system [5]. A way to mitigate the limiting effects of atmospheric turbulence and pointing errors is to employ diversity techniques, where multiple transmitting lasers and/or multiple receiving apertures are utilized [6], [7].

The performance of multiple-input multiple-output (MIMO) FSO communication links over $\mathcal{M}$ turbulence channels is scarcely investigated in the literature. Namely, the asymptotic expression for the average bit error rate (BER) of MIMO FSO links is derived in [8], while the closed-form expressions for the average BER and the outage probability (OP) of maximum ratio transmission based FSO communication systems are given in [9]. Also in [10], performance of switch-and-examine combining technique at the receiver side of a MIMO FSO communication system is presented. In addition, the average BER of maximal ratio combining technique based FSO communication systems with binary differential phase-shift keying is analysed in [11].

As a special type of orthogonal space-time block codes (STBC), Alamouti encoding scheme [12] is a technique for attaining spatial diversity in wireless fading channels. Alamouti encoding is a transmit diversity scheme that uses two antennas at the transmitter and is widely employed in RF communication systems [13] due to its simplicity. It enjoys low-complexity decoding scheme, requires the knowledge of channel state information only at the receiver side, and achieves full spatial diversity [14]. FSO communication systems employing Alamouti encoding scheme are proposed in the literature. Particularly, the average BER expression of Alamouti encoded FSO links over gamma-gamma channel with subcarrier intensity modulation/direct detection (IM/DD) is derived in [15]. Symbol error rate (SER) for Alamouti-coded FSO communication link over gamma-gamma channel with heterodyne detection (HD) is

Manuscript received October 26, 2021; revised December 7, 2021; accepted January 8, 2022. Date of publication January 13, 2022; date of current version February 1, 2022. This work was supported by Istanbul Technical University (ITU) Vodafone Future Lab under Project ITUVF20180701P09. *(Corresponding author: Abdulgani A. Ibrahim.)*

Abdulgani A. Ibrahim and Lütfiye Durak-Ata are with the Informatics Institute, Istanbul Technical University, Istanbul 34469, Turkey (e-mail: ibrahim19@itu.edu.tr; durakata@itu.edu.tr).

Serdar Özgür Ata is with the TUBITAK Informatics and Information Security Research Center, 41470 Gebze/Kocaeli, Turkey (e-mail: serdar.ata@tubitak.gov.tr).

Digital Object Identifier 10.1109/JPHOT.2022.3142682

This work is licensed under a Creative Commons Attribution 4.0 License. For more information, see https://creativecommons.org/licenses/by/4.0/

investigated in [16]. In addition, the authors in [17] extended the study in [15] by considering pointing error effects and presented SER and average capacity expressions for FSO communication systems using Alamouti encoding over gamma-gamma channels with pointing errors. Furthermore, performance of a hybrid FSO/RF communication link providing space-time diversity by using Alamouti encoding scheme or antenna selection method is studied in [18]. On the other hand, performance of Alamouti encoding scheme for the FSO communication links over $\mathcal{M}$ turbulence channels has not been studied yet in the literature, to the best of authors' knowledge.

In this study, motivated from the references given above and to fill in the gap in the current literature, we investigate the average BER and the OP performance metrics for FSO communication links employing Alamouti encoding scheme over the generalized $\mathcal{M}$ turbulence channel with pointing errors effect. In the analysis, both IM/DD and HD techniques are considered and the closed-form expressions of the average BER and the OP of the proposed system are obtained. Furthermore, asymptotic expressions for the average BER and the OP at high SNR values are given to provide more insight about the obtained results. Finally, numerical results are presented to evaluate the performance of the proposed system and show the consistency of the analytical derivations with Monte-Carlo simulations.

This paper is organized as follows: Section II first describes the system model, and then explains the assumed channel model. Also, in this section, channel's probability distribution function (PDF) is derived which is vital for the evaluation of the performance of the communication system. The average BER and the OP expressions for the proposed system are derived in Section III. In Section IV, the numerical results of the analytic derivations are given for miscellaneous values of the system parameters and verified by the simulations. Section V summarizes the results from the study and concludes the letter.

Notations: $K_v(.)$ represents the v-th order modified Bessel function of the second kind [19, Eq.(8.432)], $\Gamma[.]$ is the Gamma function [19, Eq.(8.310)], $\binom{\cdot}{\cdot}$ stands for the binomial coefficient, and $(.)^*$ denotes the complex conjugate.

II. System and Channel Models

A. System Model

We consider an FSO communication system which is employing Alamouti encoding scheme by using two transmitting apertures and one receiving aperture. We also consider both detection techniques, namely IM/DD and HD in this study. Since using Alamouti encoding method, transmitter sends it's symbols x_1 and x_2 from aperture one and aperture two, respectively, during the first transmission time interval. Further, $-x_2^*$ and x_1^* are respectively transmitted from aperture one and aperture two during the second transmission time interval. By assuming a subcarrier intensity modulation (SIM) [20] based FSO link, the received electrical symbols, r_1 and r_2 by the receiver in two consecutive time duration are given as [17]

$$[r_1\, r_2^*]^T = \eta \begin{bmatrix} h_1 & h_2 \\ h_2 & -h_1 \end{bmatrix} \begin{bmatrix} x_1 \\ x_2 \end{bmatrix} + \begin{bmatrix} z_1 \\ z_2^* \end{bmatrix}, \tag{1}$$

where η stands for optical-to-electrical conversion coefficient, h_1 and h_2 are the channel gains that account for the atmospheric turbulence and pointing error effects, and z_1 and z_2 denote the complex-valued noise components having additive white Gaussian distribution with zero-mean and σ^2 variance.

At the receiver, transmitted symbols are retrieved by multiplying $[r_1, r_2^*]^T$ in (1) with $\begin{bmatrix} h_1 & h_2 \\ h_2 & -h_1 \end{bmatrix}$ and the decoded symbols, $\tilde{x}_1$ and $\tilde{x}_2$, can be expressed as

$$\tilde{x}_i = \eta \left(h_1^2 + h_2^2\right) x_i + n_i, \;\; i = 1, 2 \tag{2}$$

where $n_1 = h_1 z_1 + h_2 z_2^*$ and $n_2 = h_2 z_1 - h_1 z_2^*$. It should be noted that HD based FSO links will require more detailed decoding procedure [16] in order to adequately take care of the phase information of different signals.

B. Channel Model

In FSO communication systems, $\mathcal{M}$ probability distribution is used to model the atmospheric turbulence effects while the statistical model for the pointing error effect is adopted from [21, Eq. (11)]. Therefore, the combined PDF of turbulence and pointing error effects is derived as [22]

$$f_h(h) = \frac{\xi^2 \mathcal{A}}{2h} \sum_{k=1}^{\beta} b_k G_{1,3}^{3,0}\left(\frac{\alpha\beta h}{(g\beta + \Omega')\, A_0} \middle| \begin{matrix} \xi^2 + 1 \\ \xi^2, \alpha, k \end{matrix} \right), \tag{3}$$

in which

$$\mathcal{A} = \frac{2\alpha^{\frac{\alpha}{2}}}{g^{1+\frac{\alpha}{2}}\Gamma[\alpha]} \left(\frac{g\beta}{g\beta + \Omega'}\right)^{\beta + \frac{\alpha}{2}}, \tag{4a}$$

$$b_k = \binom{\beta - 1}{k - 1} \frac{\alpha^{\frac{k}{2}} (g\beta + \Omega')^{1 - \frac{k}{2}} (\Omega')^{k-1}}{\beta^{\frac{k}{2}} g^{k-1} (k-1)!} \left(\frac{\alpha\beta}{g\beta + \Omega'}\right)^{-\frac{\alpha + k}{2}}, \tag{4b}$$

where $G_{p,q}^{m,n}(,|,)$ is the Meijer's G function [19], α and β are fading related parameters corresponding to the large-scale and small-scale fluctuations, respectively, in the atmospheric channel. $g = 2b_0(1-\rho)$ and $\Omega' = \Omega + \rho 2b_0 + 2\sqrt{2b_0\Omega\rho}\cos(\Phi_A - \Phi_B)$. Here, Ω is the average power of the optical signal for the line-of-sight (LOS) component, $2b_0$ is the average power of total scatter components, and ρ is the amount of the scattering power coupled to the LOS component. Further, Φ_A and Φ_B are deterministic angles for the LOS component and the coupled-to-LOS scatter component, respectively. In addition, $\xi = \frac{w_{zeq}}{2\sigma_s}$ defines the ratio between the equivalent beam radius at the receiver and the pointing error displacement standard deviation at the receiver. Also, σ_s^2 is the jitter variance at the receiver and $A_0 = (\mathrm{erf}(v))^2$ is the fraction of the collected power with zero pointing errors. $v = \frac{\sqrt{\pi}a}{\sqrt{2}w_z}$ and $w_{zeq}^2 = w_z^2 \frac{\sqrt{\pi}\,\mathrm{erf}(v)}{2v\exp(-v^2)}$. And, w_z is the beam waist at distance z and w_{zeq} is the equivalent beam waist.

After optical to electrical conversion, the instantaneous electrical SNR at the receiver can be described as [15], [16]

$$\gamma = \mu_t \underbrace{\sum_{i=1}^{2} h_i^t}_{X}, \tag{5}$$

where $\mu_t = \frac{\eta^t E^t[h]}{2N_0}$ is the average SNR [22]. Here, t defines the type of the detection technique, where $t = 1$ when HD technique is employed and $t = 2$ when IM/DD technique is used. Also, N_0 characterizes the variance of white additive Gaussian noise (AWGN) sample, and $E[.]$ denotes the expectation operator.

In order to calculate the performance metrics of the proposed FSO communication system, the PDF of X must be obtained. To do that, let's start by rewriting the Meijer's G function in (3) in terms of Hypergeometric function by using [19, Eq. (9.303)] as

$$\begin{aligned}
&G_{1,3}^{3,0}\left(\frac{\alpha\beta h}{(g\beta+\Omega')A_0}\middle|\begin{matrix}\xi^2+1\\ \xi^2,\alpha,k\end{matrix}\right)\\
&=\Gamma\left[\alpha-\xi^2\right]\Gamma\left[k-\xi^2\right]\left(\frac{\alpha\beta h}{(g\beta+\Omega')A_0}\right)^{\xi^2}\\
&\quad\times {}_1F_2\left[0;1+\xi^2-\alpha,1+\xi^2-k;\frac{\alpha\beta h}{(g\beta+\Omega')A_0}\right]\\
&\quad+\frac{\Gamma\left[\xi^2-\alpha\right]\Gamma\left[k-\alpha\right]}{\Gamma\left[1+\xi^2-\alpha\right]}\left(\frac{\alpha\beta h}{(g\beta+\Omega')A_0}\right)^{\alpha}\\
&\quad\times {}_1F_2\left[\alpha-\xi^2;1+\alpha-\xi^2,1+\alpha-k;\frac{\alpha\beta h}{(g\beta+\Omega')A_0}\right]\\
&\quad+\frac{\Gamma\left[\xi^2-k\right]\Gamma\left[\alpha-k\right]}{\Gamma\left[1+\xi^2-k\right]}\left(\frac{\alpha\beta h}{(g\beta+\Omega')A_0}\right)^{k}\\
&\quad\times {}_1F_2\left[k-\xi^2;1+k-\xi^2,1+k-\alpha;\frac{\alpha\beta h}{(g\beta+\Omega')A_0}\right].
\end{aligned}\tag{6}$$

Next, the hypergeometric functions in (6) can be expressed in terms of power series by exploiting [19, Eq. (9.14.1)] as

$$\begin{aligned}
&{}_1F_2\left[0;1+\xi^2-\alpha,1+\xi^2-k,\frac{\alpha\beta h}{(g\beta+\Omega')A_0}\right]\\
&=\sum_{j=0}^{\infty}\frac{(0)_j}{j!\left(1+\xi^2-\alpha\right)_j\left(1+\xi^2-k\right)_j}\left(\frac{\alpha\beta h}{(g\beta+\Omega')A_0}\right)^j;
\end{aligned}\tag{7a}$$

$$\begin{aligned}
&{}_1F_2\left[\alpha-\xi^2;1+\alpha-\xi^2,1+\alpha-k;\frac{\alpha\beta h}{(g\beta+\Omega')A_0}\right]\\
&=\sum_{j=0}^{\infty}\frac{\left(\alpha-\xi^2\right)_j}{j!\left(1+\alpha-\xi^2\right)_j\left(1+\alpha-k\right)_j}\left(\frac{\alpha\beta h}{(g\beta+\Omega')A_0}\right)^j;
\end{aligned}\tag{7b}$$

$$\begin{aligned}
&{}_1F_2\left[k-\xi^2;1+k-\xi^2,1+k-\alpha;\frac{\alpha\beta h}{(g\beta+\Omega')A_0}\right]\\
&=\sum_{j=0}^{\infty}\frac{\left(k-\xi^2\right)_j}{j!\left(1+k-\xi^2\right)_j\left(1+k-\alpha\right)_j}\left(\frac{\alpha\beta h}{(g\beta+\Omega')A_0}\right)^j,
\end{aligned}\tag{7c}$$

where $(k)_j$ denotes the Pochhammer symbol. Now, by plugging (6) and (7) into (3), we can obtain a power series representation of the PDF expression in (3) as

$$\begin{aligned}
f_h(h)&=\sum_{k=1}^{\beta}\frac{\xi^2\mathcal{A}b_k\Gamma\left[\alpha-\xi^2\right]\Gamma\left[k-\xi^2\right]}{2}\left(\frac{\alpha\beta}{(g\beta+\Omega')A_0}\right)^{\xi^2}\\
&\quad\times h^{\xi^2-1}\\
&+\sum_{k=1}^{\beta}\sum_{j=0}^{\infty}\frac{\xi^2\mathcal{A}b_k}{2}\frac{\Gamma\left[\xi^2-\alpha\right]\Gamma\left[k-\alpha\right]\left(\alpha-\xi^2\right)_j}{j!\Gamma\left[1+\xi^2-\alpha\right]\left(1+\alpha-\xi^2\right)_j\left(1+\alpha-k\right)_j}\\
&\quad\times\left(\frac{\alpha\beta}{(g\beta+\Omega')A_0}\right)^{\alpha+j}h^{\alpha+j-1}\\
&+\sum_{k=1}^{\beta}\sum_{j=0}^{\infty}\frac{\xi^2\mathcal{A}b_k}{2}\frac{\Gamma\left[\xi^2-k\right]\Gamma\left[\alpha-k\right]\left(k-\xi^2\right)_j}{j!\Gamma\left[1+\xi^2-k\right]\left(1+k-\xi^2\right)_j\left(1+k-\alpha\right)_j}\\
&\quad\times\left(\frac{\alpha\beta}{(g\beta+\Omega')A_0}\right)^{k+j}h^{k+j-1}.
\end{aligned}\tag{8}$$

The PDF of h^t can be obtained from (8), by employing change of variables technique, as

$$\begin{aligned}
f_{h^t}(h)&=\sum_{k=1}^{\beta}\frac{\xi^2\mathcal{A}b_k\Gamma\left[\alpha-\xi^2\right]\Gamma\left[k-\xi^2\right]}{2t}\left(\frac{\alpha\beta}{(g\beta+\Omega')A_0}\right)^{\xi^2}\\
&\quad\times h^{\frac{\xi^2-t}{t}}\\
&+\sum_{k=1}^{\beta}\sum_{j=0}^{\infty}\frac{\xi^2\mathcal{A}b_k}{2t}\frac{\Gamma\left[\xi^2-\alpha\right]\Gamma\left[k-\alpha\right]\left(\alpha-\xi^2\right)_j}{j!\Gamma\left[1+\xi^2-\alpha\right]\left(1+\alpha-\xi^2\right)_j\left(1+\alpha-k\right)_j}\\
&\quad\times\left(\frac{\alpha\beta}{(g\beta+\Omega')A_0}\right)^{\alpha+j}h^{\frac{\alpha+j-t}{t}}\\
&+\sum_{k=1}^{\beta}\sum_{j=0}^{\infty}\frac{\xi^2\mathcal{A}b_k}{2t}\frac{\Gamma\left[\xi^2-k\right]\Gamma\left[\alpha-k\right]\left(k-\xi^2\right)_j}{j!\Gamma\left[1+\xi^2-k\right]\left(1+k-\xi^2\right)_j\left(1+k-\alpha\right)_j}\\
&\quad\times\left(\frac{\alpha\beta}{(g\beta+\Omega')A_0}\right)^{k+j}h^{\frac{k+j-t}{t}}.
\end{aligned}\tag{9}$$

We then calculate the Laplace transform of h^t as

$$\begin{aligned}
M_{h^t}(s)&=\mathcal{L}\left[f_{h^t}(h)\right]=E\left[\exp\left(-sh\right)\right]\\
&=\int_0^{\infty}\exp\left(-sh\right)f_{h^t}(h)dh.
\end{aligned}\tag{10}$$

After plugging (9) into (10), the integration can be solved with the aid of [19, Eq. (3.326.2)] and we get

$$\begin{aligned}
M_{h^t}(s)&=\sum_{k=1}^{\beta}\phi_1(k)s^{\frac{-\xi^2}{t}}+\sum_{k=1}^{\beta}\sum_{j=0}^{\infty}\phi_2(k,j)s^{\frac{-\alpha-j}{t}}\\
&\quad+\sum_{k=1}^{\beta}\sum_{j=0}^{\infty}\phi_3(k,j)s^{\frac{-k-j}{t}},
\end{aligned}\tag{11}$$

where

$$\phi_1(k) = \frac{\xi^2 \mathcal{A} b_k \Gamma\left[\alpha-\xi^2\right]\Gamma\left[k-\xi^2\right]\Gamma\left[\frac{\xi^2}{t}\right]}{2t}\left(\frac{\alpha\beta}{(g\beta+\Omega')\,A_0}\right)^{\xi^2}; \tag{12a}$$

$$\phi_2(k,j) = \frac{\xi^2 \mathcal{A} b_k}{2t}\frac{\Gamma\left[\xi^2-\alpha\right]\Gamma\left[k-\alpha\right]\Gamma\left[\frac{\alpha+j}{t}\right]\left(\alpha-\xi^2\right)_j}{j!\Gamma\left[1+\xi^2-\alpha\right]\left(1+\alpha-\xi^2\right)_j\left(1+\alpha-k\right)_j} \times\left(\frac{\alpha\beta}{(g\beta+\Omega')\,A_0}\right)^{\alpha+j}; \tag{12b}$$

$$\phi_3(k,j) = \frac{\xi^2 \mathcal{A} b_k}{2t}\frac{\Gamma\left[\xi^2-k\right]\Gamma\left[\alpha-k\right]\Gamma\left[\frac{k+j}{t}\right]\left(k-\xi^2\right)_j}{j!\Gamma\left[1+\xi^2-k\right]\left(1+k-\xi^2\right)_j\left(1+k-\alpha\right)_j} \times\left(\frac{\alpha\beta}{(g\beta+\Omega')\,A_0}\right)^{k+j}. \tag{12c}$$

Now, considering an i.i.d. atmospheric channel gains for the different transmitting apertures, we can calculate the Laplace transform of X as

$$M_X(s) = \left[M_{h^t}(s)\right]^2. \tag{13}$$

In an attempt to simplify (13), let's use (11) in (13) and apply the binomial expansion twice as

$$M_X(s) = \sum_{p=0}^{2}\sum_{q=0}^{p}\binom{2}{p}\binom{p}{q}\underbrace{\left(\sum_{k=1}^{\beta}\phi_1(k)s^{\frac{-\xi^2}{t}}\right)^{2-p}}_{T_1} \times\underbrace{\left(\sum_{k=1}^{\beta}\sum_{j=0}^{\infty}\phi_2(k,j)s^{\frac{-\alpha-j}{t}}\right)^{p-q}}_{T_2}\underbrace{\left(\sum_{k=1}^{\beta}\sum_{j=0}^{\infty}\phi_3(k,j)s^{\frac{-k-j}{t}}\right)^{q}}_{T_3}. \tag{14}$$

Let's now take T_3 and start simplifying it by firstly expanding it using multinomial theorem as

$$T_3 = \sum_{\substack{v_1+v_2+\cdots+v_\beta=q\\0\le v_1,v_2,\ldots,v_\beta\le q}}\frac{q!}{v_1!v_2!\ldots v_\beta!}\left(\sum_{j=0}^{\infty}\phi_3(1,j)s^{\frac{-1-j}{t}}\right)^{v_1} \times\left(\sum_{j=0}^{\infty}\phi_3(2,j)s^{\frac{-2-j}{t}}\right)^{v_2}\ldots\left(\sum_{j=0}^{\infty}\phi_3\left(\beta,j\right)s^{\frac{-\beta-j}{t}}\right)^{v_\beta}. \tag{15}$$

Eq. (15) is further simplified by using [19, Eq. (0.314)] as

$$T_3 = \sum_{\substack{v_1+v_2+\cdots+v_\beta=q\\0\le v_1,v_2,\ldots,v_\beta\le q}}\frac{q!}{v_1!v_2!\ldots v_\beta!}\left(\sum_{j=0}^{\infty}\phi_3^{(v_1)}(1,j)s^{\frac{-v_1-j}{t}}\right) \times\left(\sum_{j=0}^{\infty}\phi_3^{(v_2)}(2,j)s^{\frac{-2v_2-j}{t}}\right)\ldots\left(\sum_{j=0}^{\infty}\phi_3^{(v_\beta)}\left(\beta,j\right)s^{\frac{-v_\beta\beta-j}{t}}\right), \tag{16}$$

where $\phi_a^{(b)}(.,.)$ denotes convolving $\phi_a(.,.)$ with itself b times. Finally, the product of power series is solved by using [19, Eq. (0.316)] as

$$T_3 = \sum_{\substack{v_1+v_2+\cdots+v_\beta=q\\0\le v_1,v_2,\ldots,v_\beta\le q}}\frac{q!}{v_1!v_2!\ldots v_\beta!}\sum_{j=0}^{\infty}\Phi_{3j}s^{\frac{-\sum_{i=1}^{\beta}v_i i-j}{t}}, \tag{17}$$

where $\Phi_{3j} = \phi_3^{(v_1)}(1,j) * \phi_3^{(v_2)}(2,j) * \cdots * \phi_3^{(v_\beta)}(\beta,j)$. Here, $*$ denotes the convolution operator. Similarly, T_1 and T_2 in (14) are simplified by taking the same steps as

$$T_1 = \sum_{\substack{r_1+r_2+\cdots+r_\beta=2-p\\0\le r_1,r_2,\ldots,r_\beta\le 2-p}}\frac{2-p!}{r_1!r_2!\ldots r_\beta!}\Phi_1 s^{\frac{-\sum_{i=1}^{\beta}r_i\xi^2}{t}}; \tag{18a}$$

$$T_2 = \sum_{\substack{u_1+u_2+\cdots+u_\beta=p-q\\0\le u_1,u_2,\ldots,u_\beta\le p-q}}\frac{p-q!}{u_1!u_2!\ldots u_\beta!}\sum_{j=0}^{\infty}\Phi_{2j}s^{\frac{-\sum_{i=1}^{\beta}u_i\alpha-j}{t}}, \tag{18b}$$

where $\Phi_1 = \phi_1^{r_1}(1)\phi_1^{r_2}(2)\ldots\phi_1^{r_{\beta-1}}(\beta-1)\phi_1^{r_\beta}(\beta)$ and $\Phi_{2j} = \phi_2^{(u_1)}(1,j) * \phi_2^{(u_2)}(2,j) * \cdots * \phi_2^{(u_\beta)}(\beta,j)$. Finally, by using (17) and (18) into (14), the simplified version of (13) can be obtained as

$$M_X(s) = \sum_{p=0}^{2}\sum_{q=0}^{p}\binom{2}{p}\binom{p}{q}\sum_{\substack{r_1+r_2+\cdots+r_\beta=2-p\\0\le r_1,r_2,\ldots,r_\beta\le 2-p}}\frac{2-p!}{r_1!r_2!\ldots r_\beta!} \times\sum_{\substack{u_1+u_2+\cdots+u_\beta=p-q\\0\le u_1,u_2,\ldots,u_\beta\le p-q}}\frac{p-q!}{u_1!u_2!\ldots u_\beta!}\sum_{\substack{v_1+v_2+\cdots+v_\beta=q\\0\le v_1,v_2,\ldots,v_\beta\le q}} \times\frac{q!}{v_1!v_2!\ldots v_\beta!} \times\sum_{j=0}^{\infty}\Psi_j s^{\frac{-\sum_{i=1}^{\beta}r_i\xi^2-\sum_{i=1}^{\beta}u_i\alpha-\sum_{i=1}^{\beta}v_i i-j}{t}}, \tag{19}$$

where $\Psi_j = \Phi_1(\Phi_{2j} * \Phi_{3j})$.

Finally, the PDF of X can be obtained by taking the inverse Laplace transform of (19) as

$$f_X(x) = \sum_{p=0}^{2}\sum_{q=0}^{p}\binom{2}{p}\binom{p}{q}\sum_{\substack{r_1+r_2+\cdots+r_\beta=2-p\\0\le r_1,r_2,\ldots,r_\beta\le 2-p}}\frac{2-p!}{r_1!r_2!\ldots r_\beta!} \times\sum_{\substack{u_1+u_2+\cdots+u_\beta=p-q\\0\le u_1,u_2,\ldots,u_\beta\le p-q}}\frac{p-q!}{u_1!u_2!\ldots u_\beta!}\sum_{\substack{v_1+v_2+\cdots+v_\beta=q\\0\le v_1,v_2,\ldots,v_\beta\le q}} \times\frac{q!}{v_1!v_2!\ldots v_\beta!}$$

$$\times \sum_{j=0}^{N} \frac{\Psi_j x^{\frac{\sum_{i=1}^{\beta} r_i\xi^2+\sum_{i=1}^{\beta} u_i\alpha+\sum_{i=1}^{\beta} v_i i+j}{t}-1}}{\Gamma\left[\frac{\sum_{i=1}^{\beta} r_i\xi^2+\sum_{i=1}^{\beta} u_i\alpha+\sum_{i=1}^{\beta} v_i i+j}{t}\right]}. \quad (20)$$

It should be noted that the upper limit of the infinite series in (19) is truncated at N terms. Now, (20) will be used to obtain the expressions of average BER and OP metrics in the next section.

III. Performance Analysis

In this section, the closed-form expressions for the average BER and the OP performance metrics are examined. In addition, corresponding asymptotic expressions for both metrics are also presented.

A. Average BER

The average BER can be evaluated as

$$\bar{P}_e = \int_0^{\infty} \mathcal{P}\left(e|\gamma\right) f_\gamma\left(\gamma\right) d\gamma, \quad (21)$$

where $\mathcal{P}(e|\gamma)$ is the conditional BER expression and it is given for the binary phase shift keying (BPSK) modulation as [23]

$$\mathcal{P}\left(e|\gamma\right) = \frac{1}{2}\operatorname{erfc}\left(\sqrt{\gamma}\right) = \frac{1}{2\sqrt{\pi}} G_{1,2}^{2,0}\left(\gamma \middle| \begin{matrix} 1 \\ 0, \frac{1}{2} \end{matrix}\right). \quad (22)$$

Also, $f_\gamma(\gamma)$ is the PDF of the received electrical SNR and it can now be easily calculated from (5) and (20) as

$$f_\gamma\left(\gamma\right) = \sum_{p=0}^{2}\sum_{q=0}^{p}\binom{2}{p}\binom{p}{q} \sum_{\substack{r_1+r_2+\cdots+r_\beta=2-p \\ 0\le r_1,r_2,\ldots,r_\beta\le 2-p}} \frac{2-p!}{r_1!r_2!\ldots r_\beta!}$$
$$\times \sum_{\substack{u_1+u_2+\cdots+u_\beta=p-q \\ 0\le u_1,u_2,\ldots,u_\beta\le p-q}} \frac{p-q!}{u_1!u_2!\ldots u_\beta!} \sum_{\substack{v_1+v_2+\cdots+v_\beta=q \\ 0\le v_1,v_2,\ldots,v_\beta\le q}}$$
$$\times \frac{q!}{v_1!v_2!\ldots v_\beta!}$$
$$\times \sum_{j=0}^{N} \frac{\Psi_j}{\Gamma\left[\frac{\sum_{i=1}^{\beta} r_i\xi^2+\sum_{i=1}^{\beta} u_i\alpha+\sum_{i=1}^{\beta} v_i i+j}{t}\right]}$$
$$\times \frac{\gamma^{\frac{\sum_{i=1}^{\beta} r_i\xi^2+\sum_{i=1}^{\beta} u_i\alpha+\sum_{i=1}^{\beta} v_i i+j}{t}-1}}{\mu_t^{\frac{\sum_{i=1}^{\beta} r_i\xi^2+\sum_{i=1}^{\beta} u_i\alpha+\sum_{i=1}^{\beta} v_i i+j}{t}}}. \quad (23)$$

Now, by substituting (22) and (23) into (21) and solving the integration with the aid of [24, Eq. (07.34.21.0009.01)], the average BER can be derived in a closed-form as

$$\bar{P}_e = \sum_{p=0}^{2}\sum_{q=0}^{p}\binom{2}{p}\binom{p}{q} \sum_{\substack{r_1+r_2+\cdots+r_\beta=2-p \\ 0\le r_1,r_2,\ldots,r_\beta\le 2-p}} \frac{2-p!}{r_1!r_2!\ldots r_\beta!}$$
$$\times \sum_{\substack{u_1+u_2+\cdots+u_\beta=p-q \\ 0\le u_1,u_2,\ldots,u_\beta\le p-q}} \frac{p-q!}{u_1!u_2!\ldots u_\beta!} \sum_{\substack{v_1+v_2+\cdots+v_\beta=q \\ 0\le v_1,v_2,\ldots,v_\beta\le q}}$$
$$\times \frac{q!}{v_1!v_2!\ldots v_\beta!}$$
$$\times \sum_{j=0}^{N} \frac{\Psi_j}{2\sqrt{\pi}\Gamma\left[\frac{\sum_{i=1}^{\beta} r_i\xi^2+\sum_{i=1}^{\beta} u_i\alpha+\sum_{i=1}^{\beta} v_i i+j}{t}+1\right]}$$
$$\times \frac{\Gamma\left[\frac{\sum_{i=1}^{\beta} r_i\xi^2+\sum_{i=1}^{\beta} u_i\alpha+\sum_{i=1}^{\beta} v_i i+j}{t}+\frac{1}{2}\right]}{\mu_t^{\frac{\sum_{i=1}^{\beta} r_i\xi^2+\sum_{i=1}^{\beta} u_i\alpha+\sum_{i=1}^{\beta} v_i i+j}{t}}}. \quad (24)$$

At high SNR values ($\mu_t \to \infty$), the term with the smallest exponent which corresponds to the first term of the infinite series (when $j = 0$) will dominate (24). Thus, by setting $j = 0$ in (24), the asymptotic average BER can be obtained as

$$\bar{P}_e^{\infty} \approx \sum_{p=0}^{2}\sum_{q=0}^{p}\binom{2}{p}\binom{p}{q} \sum_{\substack{r_1+r_2+\cdots+r_\beta=2-p \\ 0\le r_1,r_2,\ldots,r_\beta\le 2-p}} \frac{2-p!}{r_1!r_2!\ldots r_\beta!}$$
$$\times \sum_{\substack{u_1+u_2+\cdots+u_\beta=p-q \\ 0\le u_1,u_2,\ldots,u_\beta\le p-q}}$$
$$\times \frac{p-q!}{u_1!u_2!\ldots u_\beta!} \sum_{\substack{v_1+v_2+\cdots+v_\beta=q \\ 0\le v_1,v_2,\ldots,v_\beta\le q}} \frac{q!}{v_1!v_2!\ldots v_\beta!}$$
$$\times \frac{\Psi_0\Gamma\left[\frac{\sum_{i=1}^{\beta} r_i\xi^2+\sum_{i=1}^{\beta} u_i\alpha+\sum_{i=1}^{\beta} v_i i}{t}+\frac{1}{2}\right]}{2\sqrt{\pi}\Gamma\left[\frac{\sum_{i=1}^{\beta} r_i\xi^2+\sum_{i=1}^{\beta} u_i\alpha+\sum_{i=1}^{\beta} v_i i}{t}+1\right]}$$
$$\times \mu_t^{-\frac{\sum_{i=1}^{\beta} r_i\xi^2+\sum_{i=1}^{\beta} u_i\alpha+\sum_{i=1}^{\beta} v_i i}{t}}. \quad (25)$$

Here, $\Psi_0 = \Phi_1\Phi_2\Phi_3$, where Φ_2 and Φ_3 are given as $\Phi_2 = \phi_2^{u_1}(1,0)\phi_2^{u_2}(2,0)\ldots\phi_2^{u_{\beta-1}}(\beta-1,0)\phi_2^{u_\beta}(\beta,0)$ and $\Phi_3 = \phi_3^{v_1}(1,0)\phi_3^{v_2}(2,0)\ldots\phi_3^{v_{\beta-1}}(\beta-1,0)\phi_3^{v_\beta}(\beta,0)$.

B. Outage Probability

The outage probability of a communication system is defined as the probability that the received instantaneous SNR is smaller than a predefined threshold, γ_{th}, and it can be expressed as

$$P_{out} = \mathcal{P}\left[\gamma < \gamma_{th}\right] = F_\gamma\left(\gamma_{th}\right), \quad (26)$$

where $F_\gamma(\gamma_{th})$ is the CDF of γ which can be obtained from (23) as

$$F_\gamma\left(\gamma_{th}\right) = \sum_{p=0}^{2}\sum_{q=0}^{p}\binom{2}{p}\binom{p}{q} \sum_{\substack{r_1+r_2+\cdots+r_\beta=2-p \\ 0\le r_1,r_2,\ldots,r_\beta\le 2-p}} \frac{2-p!}{r_1!r_2!\ldots r_\beta!}$$
$$\times \sum_{\substack{u_1+u_2+\cdots+u_\beta=p-q \\ 0\le u_1,u_2,\ldots,u_\beta\le p-q}}$$
$$\times \frac{p-q!}{u_1!u_2!\ldots u_\beta!} \sum_{\substack{v_1+v_2+\cdots+v_\beta=q \\ 0\le v_1,v_2,\ldots,v_\beta\le q}} \frac{q!}{v_1!v_2!\ldots v_\beta!}$$

$$\times \sum_{j=0}^{N} \frac{\Psi_j}{\Gamma\left[\frac{\sum_{i=1}^{\beta} r_i\xi^2+\sum_{i=1}^{\beta} u_i\alpha+\sum_{i=1}^{\beta} v_i i+j}{t}+1\right]} \times \left(\frac{\gamma_{th}}{\mu_t}\right)^{\frac{\sum_{i=1}^{\beta} r_i\xi^2+\sum_{i=1}^{\beta} u_i\alpha+\sum_{i=1}^{\beta} v_i i+j}{t}}. \quad (27)$$

Furthermore, the asymptotic OP can be obtained as

$$P_{out}^{\infty} \approx \sum_{p=0}^{2}\sum_{q=0}^{p}\binom{2}{p}\binom{p}{q} \sum_{\substack{r_1+r_2+\cdots+r_\beta=2-p \\ 0\le r_1,r_2,\ldots,r_\beta\le 2-p}} \frac{2-p!}{r_1!r_2!\ldots r_\beta!} \times \sum_{\substack{u_1+u_2+\cdots+u_\beta=p-q \\ 0\le u_1,u_2,\ldots,u_\beta\le p-q}} \frac{p-q!}{u_1!u_2!\ldots u_\beta!} \sum_{\substack{v_1+v_2+\cdots+v_\beta=q \\ 0\le v_1,v_2,\ldots,v_\beta\le q}} \frac{q!}{v_1!v_2!\ldots v_\beta!} \times \frac{\Psi_0}{\Gamma\left[\frac{\sum_{i=1}^{\beta} r_i\xi^2+\sum_{i=1}^{\beta} u_i\alpha+\sum_{i=1}^{\beta} v_i i}{t}+1\right]} \times \left(\frac{\gamma_{th}}{\mu_t}\right)^{\frac{\sum_{i=1}^{\beta} r_i\xi^2+\sum_{i=1}^{\beta} u_i\alpha+\sum_{i=1}^{\beta} v_i i}{t}}. \quad (28)$$

IV. Numerical Results and Simulations

In this section, we present numerical results of the derived expressions for the average BER and OP of FSO communication systems employing Alamouti encoding scheme over $\mathcal{M}$ turbulence channel with pointing error effects. To verify the accuracy of the analytic derivations, Monte-Carlo simulations are provided for miscellaneous system parameters and their various values are given as $\Omega = 1.3265$, $b_0 = 0.1079$, $\rho = 0.596$, and $\Phi_A - \Phi_B = \frac{\pi}{2}$. Additionally, the values of α and β parameters are set as $\alpha = 2.296, \beta = 2$ for strong turbulence, $\alpha = 4.2, \beta = 3$ for medium turbulence, and $\alpha = 8.1, \beta = 4$ for weak turbulence levels.[1]

In Fig. 1, the average BER performance of the proposed system is presented by consedering both IM/DD and HD detection techniques with different levels of pointing errors effect, such that the parameter value of $\xi = 6.7$ indicating weak pointing errors effect, $\xi = 1.45$ for moderate pointing errors level, and $\xi = 1.1$ indicating strong pointing errors effect. From the figure, it is seen that the average BER performance metric declines with the increase of severity of pointing errors effect. For example, to achieve the average BER value of 10^{-6}, SNR requirement is approximately 5 dB higher for the link under strong pointing errors level than the link under weak pointing errors level when the HD method is used for signal detection. The figure also shows that a link employing HD signal detection technique outperforms the link using IM/DD technique. For example, at 25 dB SNR value, HD technique provides 10^{-6} average BER value while this error performance value has just 10^{-3} value when using IM/DD technique. Furthermore, the figure presents that the asymptotic average BER expression converges to the closed-form expression in high SNR region as expected.

[1]The values of the simulation parameters are obtained from [25], [26], and they are used just to validate the derived analytical expressions. Different values of the parameters can be chosen if deemed more appropriate for a system design.

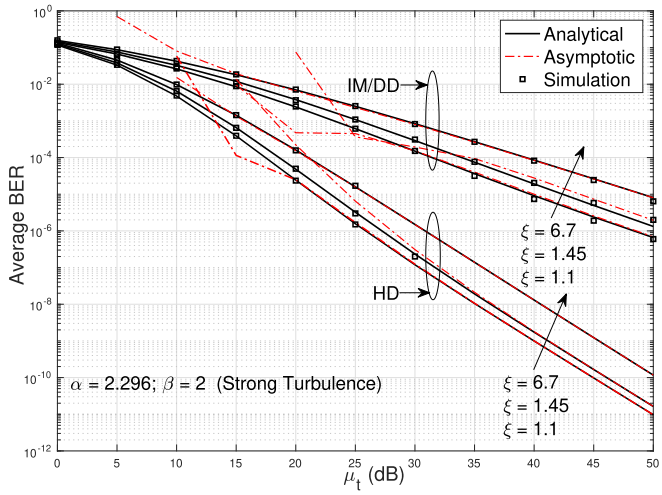

Fig. 1. Average BER performance of FSO links with Alamouti encoding under strong, moderate, and weak pointing error levels.

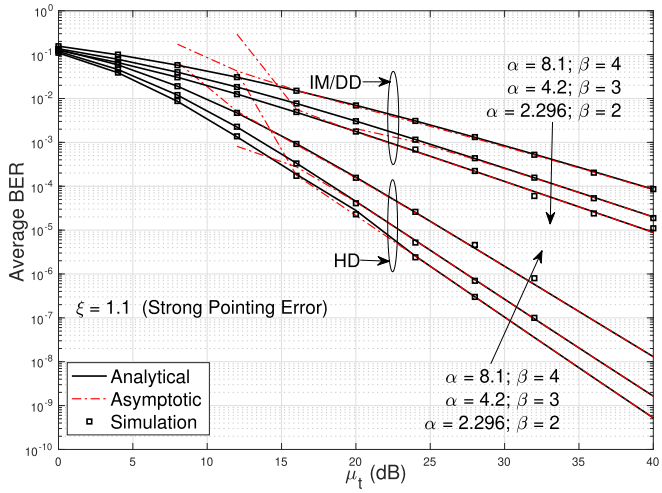

Fig. 2. Average BER performance of FSO links with Alamouti encoding under different severity of atmospheric turbulence effects.

Fig. 2 illustrates the average BER performance metrics of Alamouti encoded FSO communication systems under the influence of weak, moderate, and strong atmospheric turbulence regimes. The figure shows that a decrease in the atmospheric turbulence level enhances the performance of the communication system, as expected. As an example, at an average SNR of 28 dB, a HD technique based FSO link under moderate turbulence level yields an average BER value of 7×10^{-7}, while a similar link under strong turbulence level gives an average BER value of 3.84×10^{-6}.

Fig. 3 presents the average BER performance enhancement obtained by using the Alamouti encoding scheme in the FSO

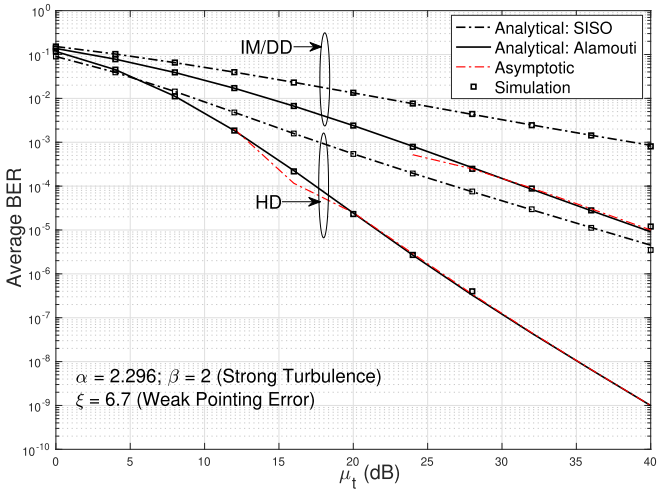

Fig. 3. Comparison of the average BER performance of FSO communication links with and without Alamouti encoding scheme.

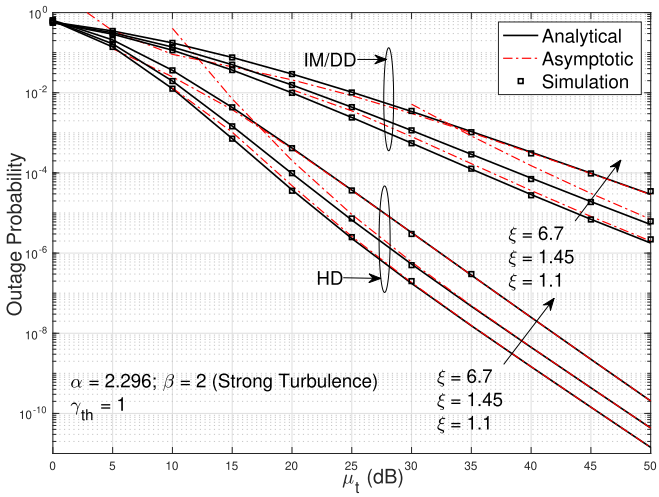

Fig. 4. Outage probability performance of FSO links with Alamouti encoding under strong, moderate, and weak pointing error levels.

communication systems over $\mathcal{M}$ turbulence channels. To conduct a fair comparison, the total transmitted power of the SISO FSO system and the total transmitted power of the Alamouti based FSO system are kept the same. It can be seen from the figure that the FSO links with Alamouti encoding abundantly outperform the FSO links with only a single transmitting aperture. For instance, at an average SNR of 20 dB, an FSO link with Alamouti encoding yields an average BER value of 2.31×10^{-5} while the average BER becomes 5.4×10^{-4} at the FSO link without Alamouti scheme, when HD signal detection technique is used. Since the total transmitted power of both systems are the same, the acquired performance improvement is just because of the diversity gain obtained from the employment of Alamouti encoding shceme.

The OP performance of Alamouti encoded FSO communication systems over $\mathcal{M}$ channels is depicted in Fig. 4. Here the plots are given for both IM/DD and HD detection techniques and

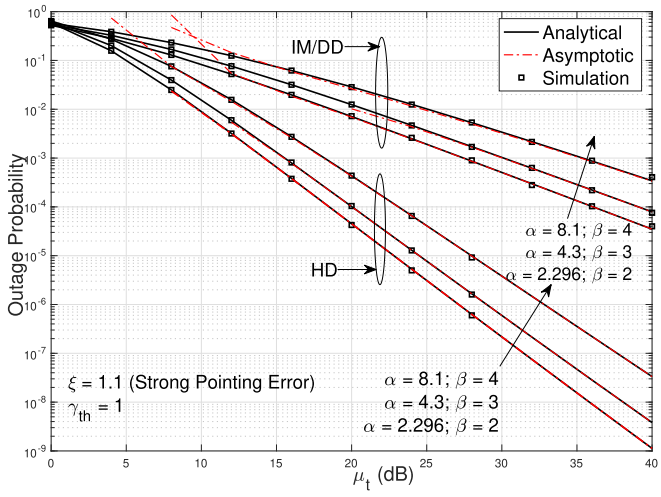

Fig. 5. Outage probability performance of FSO links employing Alamouti encoding under different severity of atmospheric turbulence effects.

show the OP performances of the proposed system for strong, moderate, and weak pointing error circumstances while keeping the atmospheric turbulence effect constant. It can be observed from the figure that the pointing errors significantly degrade the OP performance of the FSO systems and increasing the severity level of the pointing errors worsens the OP performance even in high SNR region. For example, at 35 dB SNR and when IM/DD technique is employed, the OP becomes 10^{-4} in the case of weak point errors, while on the other hand it has a value of 10^{-3} for the case of strong pointing errors. Also, it is shown that an FSO link that uses HD signal detection technique is outperforming a one with IM/DD technique, such that in order to obtain an OP value of 2.2×10^{-6}, the HD technique provides an SNR gain of about 25 dB over the IM/DD technique. Furthermore, it can be seen from the figure that the asymptotic expressions quickly converge with the analytical expressions at high SNR values.

Fig. 5 shows the OP performance of FSO communication systems employing Alamouti encoding scheme over $\mathcal{M}$ channels. Here the results are presented for varying atmospheric turbulence effects while assuming the pointing error effects constant. It can be easily seen that OP performance deteriorates with the increase of the atmospheric turbulence effect. As an example, at an average SNR of 32 dB, an IM/DD technique based Alamouti encoded FSO link yields an OP value of 6.3×10^{-4} under medium turbulence effect, while the same link has an OP value of 2.1×10^{-3} under strong turbulence effect.

Fig. 6 compares the OP performance metrics of FSO links with and without Alamouti encoding scheme. Strong atmospheric turbulence and weak pointing error levels are assumed in this figure. Here again, the total transmitted power for both systems are kept equal for a fair comparison. It's evident from the figure that a better OP performance is achieved with the Alamouti encoded FSO links. For instance, a HD technique based Alamouti encoded FSO link has 4.44×10^{-4} value of OP at an average SNR of 16 dB, while its counterpart link without Alamouti encoding scheme gives an OP value of 5.9×10^{-3}.

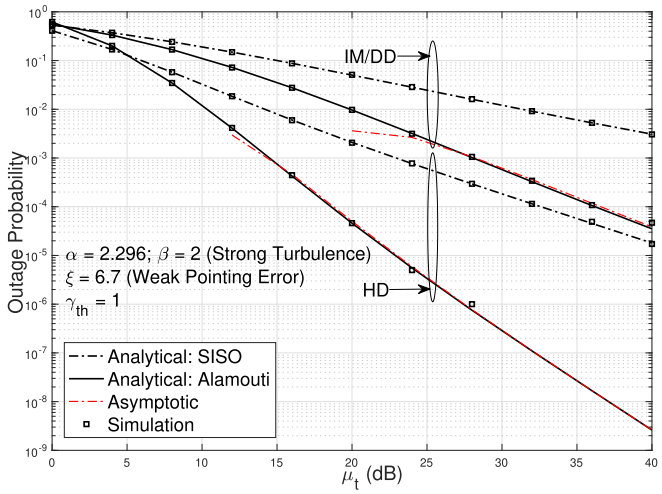

Fig. 6. Comparison of outage probability performance of FSO communication links with and without Alamouti encoding scheme.

V. Conclusion

In this paper, Alamouti encoding scheme is proposed to be employed in FSO communication systems to combat the atmospheric turbulence and pointing errors effects, and thus increase the reliability of the entire system. In the considered system model, FSO links are assumed to be over $\mathcal{M}$ channel which is a general form of several channel models such as gamma-gamma channels, K channels or negative exponential channels. Therefore the obtained results are also valid for all these channel models. To examine the performance of the proposed system, first the PDF of the sum of $\mathcal{M}$ distributed fading channel gains are derived in the presence of pointing errors effect. Then, the closed-form and asymptotic expressions of the average BER and OP metrics are obtained for Alamouti encoded FSO communication systems. Furthermore, the correctness of the analytic derivations are verified with Monte-Carlo simulations. Additionally, performance improvement of FSO communication links is illustrated by the numerical and simulation results when Alamouti encoding scheme is applied. It is also shown with the numerical results how atmospheric turbulence and pointing errors negatively affect the performance of FSO communication links. Finally, the results highlight that HD detection technique based FSO links outperform IM/DD detection based FSO links.

References

[1] M. Alzenad, M. Z. Shakir, H. Yanikomeroglu, and M.-S. Alouini, "FSO-based vertical backhaul/fronthaul framework for 5G wireless networks," *IEEE Commun. Mag.*, vol. 56, no. 1, pp. 218–224, Jan. 2018.

[2] A. S. Hamza, J. S. Deogun, and D. R. Alexander, "Classification framework for free space optical communication links and systems," *IEEE Commun. Surveys Tuts.*, vol. 21, no. 2, pp. 1346–1382, Apr.–Jun. 2018.

[3] S. A. Al-Gailani *et al.*, "A survey of free space optics (FSO) communication systems, links, and networks," *IEEE Access*, vol. 9, pp. 7353–7373, 2021.

[4] A. A. Ibrahim, S. Ata, E. Erdoğan, and L. Durak-Ata, "Performance analysis of free space optical communication systems over imprecise Málaga fading channels," *Opt. Commun.*, vol. 457, 2020, Art. no. 124694.

[5] C. Peng *et al.*, "Modeling and correction of pointing errors in gimbals-type optical communication terminals on motion platforms," *IEEE Photon. J.*, vol. 13, no. 3, Jun. 2021, Art. no. 6600915.

[6] S. Jiang *et al.*, "Performance analysis of space-diversity free-space optical links over exponentiated Weibull channels," *IEEE Photon. Technol. Lett.*, vol. 27, no. 21, pp. 2250–2252, Nov. 2015.

[7] J. Zhang, L. Dai, Y. Han, Y. Zhang, and Z. Wang, "On the ergodic capacity of MIMO free-space optical systems over turbulence channels," *IEEE J. Sel. Areas Commun.*, vol. 33, no. 9, pp. 1925–1934, Sep. 2015.

[8] D. Chen, G. Huang, G. Liu, and Y. Lei, "Performance of adaptive sub-carrier modulated MIMO wireless optical communications in Málaga turbulence," *Opt. Commun.*, vol. 435, pp. 265–270, 2019.

[9] A. A. Ibrahim and T. Gucluoglu, "Performance analysis of maximum ratio transmission based FSO link over Málaga turbulence channel," *Opt. Commun.*, vol. 450, pp. 341–346, 2019.

[10] A. Das, B. Bag, C. Bose, and A. Chandra, "Free space optical links over Málaga turbulence channels with transmit and receive diversity," *Opt. Commun.*, vol. 456, 2020, Art. no. 124591.

[11] N. D. Milosevic, M. I. Petkovic, and G. T. Djordjevic, "Average BER of SIM-DPSK FSO system with multiple receivers over $\mathcal{M}$-distributed atmospheric channel with pointing errors," *IEEE Photon. J.*, vol. 9, no. 4, Aug. 2017, Art. no. 6601210.

[12] S. M. Alamouti, "A simple transmit diversity technique for wireless communications," *IEEE J. Sel. Areas Commun.*, vol. 16, no. 8, pp. 1451–1458, Oct. 1998.

[13] T.-H. Liu, "Analysis of the Alamouti STBC MIMO system with spatial division multiplexing over the Rayleigh fading channel," *IEEE Trans. Wireless Commun.*, vol. 14, no. 9, pp. 5156–5170, Sep. 2015.

[14] F. J. Lopez-Martinez, E. Martos-Naya, K.-K. Wong, and J. T. Entrambasaguas, "Closed-form BER analysis of Alamouti-MRC systems with ICSI in Ricean fading channels," *IEEE Commun. Lett.*, vol. 15, no. 1, pp. 46–48, Jan. 2011.

[15] J. Park, E. Lee, and G. Yoon, "Average bit-error rate of the Alamouti scheme in gamma-gamma fading channels," *IEEE Photon. Technol. Lett.*, vol. 23, no. 4, pp. 269–271, Feb. 2011.

[16] M. Niu, J. Cheng, and J. F. Holzman, "Alamouti-type STBC for atmospheric optical communication using coherent detection," *IEEE Photon. J.*, vol. 6, no. 1, Feb. 2014, Art. no. 7900217.

[17] M. R. Bhatnagar and S. Anees, "On the performance of Alamouti scheme in gamma-gamma fading FSO links with pointing errors," *IEEE Wireless Commun. Lett.*, vol. 4, no. 1, pp. 94–97, Feb. 2015.

[18] M. A. Amirabadi and V. T. Vakili, "Performance analysis of hybrid FSO/RF communication systems with Alamouti coding or antenna selection," *J. Eng.*, vol. 2019, no. 5, pp. 3433–3437, 2019.

[19] I. S. Gradshteyn and I. M. Ryzhik, *Table of Integrals, Series, and Products*. San Diego, CA, USA: Academic, 2014.

[20] W. O. Popoola and Z. Ghassemlooy, "BPSK subcarrier intensity modulated free-space optical communications in atmospheric turbulence," *J. Lightw. Technol.*, vol. 27, no. 8, pp. 967–973, 2009.

[21] A. A. Farid and S. Hranilovic, "Outage capacity optimization for free-space optical links with pointing errors," *J. Lightw. Technol.*, vol. 25, no. 7, pp. 1702–1710, 2007.

[22] I. S. Ansari, F. Yilmaz, and M.-S. Alouini, "Performance analysis of free-space optical links over Málaga turbulence channels with pointing errors," *IEEE Trans. Wireless Commun.*, vol. 15, no. 1, pp. 91–102, Jan. 2016.

[23] J. Lu, K. B. Letaief, J.-I. Chuang, and M. L. Liou, "M-PSK and M-QAM BER computation using signal-space concepts," *IEEE Trans. Commun.*, vol. 47, no. 2, pp. 181–184, Feb. 1999.

[24] "From Wolfram research, The mathematical functions site," 2001. [Online]. Available: http://functions.wolfram.com

[25] S. H. Islam *et al.*, "Impact of correlation and pointing error on secure outage performance over arbitrary correlated Nakagami-m and $\mathcal{M}$-turbulent fading mixed RF-FSO channel," *IEEE Photon. J.*, vol. 13, no. 2, Apr. 2021, Art. no. 7900117.

[26] R. Singh, M. Rawat, and A. Jaiswal, "On the physical layer security of mixed FSO-RF SWIPT system with non-ideal power amplifier," *IEEE Photon. J.*, vol. 13, no. 4, Aug. 2021, Art. no. 7300517.